Journal of Inflammation Research Dovepress

Open Access Full Text Article ORIGINAL RESEARCH

Bioinformatics Identification and Validation of Ferroptosis-Related Key Genes and Therapeutic Compounds in Septic Lung Injury

Zhile Li, Han Gan, Siyuan Li, Yuchen Xue, Kai Luo, Kai Huang, Yunqian Zhang, Yan Wang, Lai Jiang, Hui Zhang

Department of Anesthesiology and Surgical Intensive Care Unit, Xinhua Hospital Affiliated to Shanghai Jiao Tong University School of Medicine, Shanghai, People's Republic of China

Correspondence: Lai Jiang; Hui Zhang, Department of Anesthesiology and Surgical Intensive Care Unit, Xinhua Hospital Affiliated to Shanghai Jiao Tong University School of Medicine, 1665 Kongjiang Road, Shanghai, 200092, People's Republic of China, Email jianglai@xinhuamed.com.cn; zhanghui22002@xinhuamed.com.cn

Background: Septic lung injury (SLI) is a severe condition with high mortality, and ferroptosis, a form of programmed cell death, is implicated in its pathogenesis. However, the explicit mechanisms underlying this condition remain unclear. This study aimed to elucidate and validate key ferroptosis-related genes involved in the pathogenesis of SLI through bioinformatics analysis and experimental validation.

Methods: Microarray data related to SLI from the GSE130936 dataset were downloaded from the Gene Expression Omnibus (GEO) database. These data were then intersected with the FerrDb database to obtain ferroptosis-related differentially expressed genes (DEGs). Protein-protein interaction (PPI) networks and functional enrichment analysis were employed to identify key ferroptosis-related DEGs. The Connectivity Map (c-MAP) tool was used to search for potential compounds or drugs that may inhibit ferroptosis-related DEGs. The transcriptional levels of the key genes and potential therapeutic compounds were verified in an LPS-induced mouse model of lung injury. The expression of these key genes was further verified using the GSE60088 and GSE137342 datasets.

Results: 38 ferroptosis-related DEGs were identified between the septic and control mice. PPI network analysis revealed four modules, the most significant of which included eight ferroptosis-related DEGs. Functional enrichment analysis showed that these genes were enriched in the HIF-1 signaling pathway, including IL-6 (Interleukin-6), TIMP1 (Tissue Inhibitor of Metalloproteinase 1), HIF-1α (Hypoxia-Inducible Factor-1α), and HMOX1 (Heme Oxygenase-1). Phloretin, a natural compound, was identified as a potential inhibitor of these genes. Treatment with phloretin significantly reduced the expression of these genes ($p < 0.05$), mitigated lung injury, improved inflammatory profiles by approximately 50%, and ferroptosis profiles by nearly 30% in the SLI models.

Conclusion: This study elucidates the significant role of ferroptosis in SLI and identifies phloretin as a potential therapeutic agent. However, further research, particularly involving human clinical trials, is necessary to validate these findings for clinical use.

Keywords: sepsis, SLI, ferroptosis, bioinformatics, HIF-1α, phloretin

Introduction

Sepsis refers to lethal organ dysfunction caused by a dysregulated host response to infection, and is a major cause of morbidity and mortality in ICU patients.[1] Among the organs involved, the lungs are the most susceptible to infection,[2] and septic patients are prone to developing acute lung injury (ALI) or acute respiratory distress syndrome (ARDS), which leads to a high mortality rate of > 30%.[3] Therefore, it is important to explore innovative mechanisms and pharmacological interventions for septic lung injury (SLI) to improve patient survival.

Regulated cell death (RCD) includes pyroptosis, apoptosis, ferroptosis, and regulated necrosis (necroptosis), all of which are involved in sepsis and organ dysfunction.[4] Among these, ferroptosis, a unique form of programmed cell death

Received: 2 May 2024
Accepted: 26 October 2024
Published: 21 November 2024

characterized by abnormal iron metabolism and excessive lipid peroxidation,[5] has emerged as an academic point of interest among researchers. Recent studies have confirmed its contribution to a range of diseases, including cancer, ischemic diseases, infections, and immune system disorders.[5–7] Recent studies have explored the role of ferroptosis in ALI development of acute lung injury. For instance, ferroptosis has been identified as a crucial form of cell death in a lipopolysaccharide (LPS)-induced lung injury model,[8] and numerous ferroptosis-related key molecules and pathways have been identified in ALI caused by various factors.[9] Notable work by Zhang et al explored the regulatory mechanisms of neutrophils and ferroptosis in SLI.[10] Moreover, specific proteins such as MUC1 and AUF1 have been identified as crucial for mitigating ferroptosis-related SLI.[11,12] Relevant therapeutic targets are also being explored and studied. Esketamine was found to alleviate ferroptosis-mediated lipid peroxidation via upregulation of HIF-1α/HO-1 pathway in acute lung injury.[13] Similarly, another study on acute lung injury revealed that sodium houttuyniae, an herbaceous plant, mitigated ferroptosis by through TRAF6-c-Myc signaling pathway.[14] In addition, the activation of AMPK/Nrf-2 signaling pathway by upregulation of GPX4 (glutathione peroxidase 4) and SLC7A11 (solute carrier family 7 member 11) could inhibit ferroptosis in lung ischemia-reperfusion injury.[15]

Phloretin, a hydrolysis product of phlorizin derived from apple plants, exhibits numerous pharmacological properties including anticancer, antibacterial, and anti-inflammatory effects.[16] Crucially, both in vivo and in vitro experiments have demonstrated that phloretin alleviates acute lung injury by reducing the production of inflammatory factors, blocking the NF-κB and MAPK pathways, and inhibiting glycolysis in macrophage.[17] However, the specific mechanisms underlying the role of phloretin in attenuation of ferroptosis during SLI remain unclear.

Bioinformatics analysis (BA) uses clustering and statistics to reveal interdependent relationships between molecules, genes, and pathways.[18] Researchers have utilized BA in fields of ischemic stroke, aortic valve disease and osteoporosis[19–21] to explore key genes related to diseases. Interestingly, HMOX1, SLC2A3, IL-6 and HIF-1α are frequently enriched as hub genes in similar studies. Such study approach not only enhances the reliability of the results but also provides new insights for disease diagnosis and treatment. However, studies of ferroptosis-related SLI are lacking. By analyzing the Gene Expression Omnibus (GEO) microarray database and intersecting it with the FerrDB database, we identified ferroptosis-related differentially expressed genes (DEGs) and conducted functional enrichment analyses. After validating the expression of hub genes in other datasets, the Connectivity Map (c-MAP) database was used to identify whether phloretin may affect key DEGs of ferroptosis during SLI. Finally, we established SLI animal models by intraperitoneal administration of LPS, and phloretin was used to verify its therapeutic effects in SLI. This study sheds light on the nascent molecular mechanisms and intervention strategies for ferroptosis-related SLI.

Materials and Methods

Microarray Data

We visited the GEO database (https://www.ncbi.nlm.nih.gov/geo/) and downloaded transcriptome data from SLI-related microarray datasets (GSE130936, GSE60088, and GSE137342). The search terms used were "sepsis-lung". The GSE130936 dataset was analyzed with the Affymetrix Mouse Expression 430A Array, in which we used the expression profile data in lung samples harvested from mice 22 h after challenge with either saline as a control (n = 4) or LPS (n = 3) as a sepsis model.

Differentially Expressed Gene Analysis

We used GEO2R (https://www.ncbi.nlm.nih.gov/geo/geo2r/) to compare the gene expression data between the LPS and Control group in the GSE130936 dataset with $p_{adjusted} < 0.05$ and $|\log_2 FC| > 1$ as the threshold. Ferroptosis-related genes (including drivers, suppressors, and markers) were obtained from the FerrDb database (www.zhounan.org/ferrdb/index.html/). Finally, these genes were intersected with the DEGs of the GSE130936 dataset to identify ferroptosis-related DEGs.

Functional Enrichment Analysis

The ClusterProfiler package, org. The Hs.eg.db package and the Gene ontology GO plot package were loaded into R software to perform Gene ontology (GO) and Kyoto Encyclopedia of Genes and Genomes (KEGG) analyses on ferroptosis-related DEGs ($p < 0.05$).

PPI Network Analysis

Ferroptosis-related DEGs were uploaded to the Search Tool for the Retrieval of Interacting Genes/Proteins (STRING) database (www.string-db.org/) to predict the PPI networks (interaction score > 0.4). The results were then imported into Cytoscape software v.3.9.1, and the Molecular Complex Detection (MCODE) plugin was used to perform clustering analyses of the ferroptosis-related DEGs (Degree Cutoff = 2, Node Score Cutoff = 0.2, K-Core = 2, and Max. Depth = 100).

Molecular Docking

To analyze the binding affinities and modes of interaction between the drug candidate and their targets, AutodockVina 1.2.2, a silico protein–ligand docking software was employed.[22] The molecular structures of phloretin was retrieved from PubChem Compound (https://pubchem.ncbi.nlm.nih.gov/).[23] The 3D coordinates of L-6, TIMP1, HIF-1α and HMOX1 were downloaded from the PDB (http://www.rcsb.org/pdb/home/home.do). Molecular docking studies were performed by Autodock Vina 1.2.2 (http://autodock.scripps.edu/).

Animal Experiments and Grouping

Male Institute of Cancer Research (ICR) mice (weighing 25–30 g) were used in this study. Animals were kept in an environmentally controlled room (temperature, 24 ± 2°C; humidity, 55 ± 10%) with a 12 h light/dark cycle and free access to food and water. All experimental procedures were approved by the Animal Ethics Committee of Xinhua Hospital, Shanghai Jiao Tong University School of Medicine. Eighteen mice were randomly assigned to three groups: control (Con), LPS, and LPS + phloretin (LPS + PHL), each comprising six mice. Phloretin (CAS No. 60-82-2, MCE) was dissolved in dimethyl sulfoxide (DMSO) to a concentration of 2.5 mg/mL. Mice from the LPS + Ph group were injected intraperitoneally with the prepared phloretin (20 mg/kg) solution seven days in a row before LPS treatment. The phloretin solution was replaced with DMSO in the control and LPS groups. LPS (L2630, Sigma-Aldrich, St. Louis, MO, United States, 5 mg/kg) was intraperitoneally injected after 7 days of PHL pretreatment and the mice were sacrificed 24 h later. Animal studies were performed in accordance with the Guide for the Care and Use of Laboratory Animals published by the NIH (NIH publication No.85–23, revised 1996).

ELISA Analysis

24 hours after LPS treatment, blood samples were collected from the mice by cardiac puncture, centrifuged at 3000 rpm for 5 min, and the supernatant was stored at −80°C before use. Serum concentrations of TNF-α (Cusabio Biotech, Wuhan, China) and IL-6 (Cusabio Biotech) were measured using ELISA kits according to the manufacturer's instructions. All samples were run in triplicate.

Histology

The left lower lobes of the lung specimens were fixed with 10% formalin, embedded in paraffin, and cut into 4 μm sections. The lung tissue was stained with hematoxylin and eosin, and histopathological changes were visualized using light microscopy (Olympus, Tokyo, Japan). The degree of lung injury was analyzed by two pathologists who were blinded to the study based on a scoring system described in a previous study.[24]

Immunofluorescence of 8-OH-dG

Paraffin sections (4 μm) of lung tissues were rehydrated and microwaved to retrieve antigens. After incubation with 5% BSA for 1 h, the sections were incubated with primary antibodies against 8-hydroxy-2′-deoxyguanosine (8-OHdG) (Abcam, 1:200, Cambridge, MA, USA) overnight. Subsequently, the sections were incubated with secondary antibodies (Alexa Fluor 488: goat anti-mouse, 1:400, Servicebio, Wuhan, China) in the dark for 1 h and counterstained with 4′,6-diamidino-2-phenylindole (DAPI) (Beyotime). The stained slices were observed under a fluorescence microscope (Nikon, Tokyo, Japan).

TdT-Mediated dUTP Nick-End Labeling (TUNEL) Assay

Lung samples used for immunofluorescence analysis were used for the TUNEL assay. Apoptotic staining was performed according to the manufacturer's protocol (Beyotime). DAPI staining was performed to determine the number of nuclei present. TUNEL signals were observed under a fluorescence microscope (Nikon, Tokyo, Japan).

Malondialdehyde Detection

A lipid peroxidation malondialdehyde assay kit (Beyotime) was used to measure the MDA content in the lungs, following the manufacturer's instructions. The absorbance was measured at 532 nm (n = 6 per group).

Detection of Glutathione Disulfide

Oxidized GSSG is a common marker for measuring levels of oxidative stress. The GSSG levels in the lungs were quantified using a detection kit (Beyotime). Absorbance was measured at 412 nm (n = 6 per group).

Western Blotting

Proteins were extracted from the lung tissues using a mixture of cold RIPA lysis buffer (Beyotime). Equal amounts of samples (40 μg) were resolved by electrophoresis on 10% or 15% SDS sulfate-polyacrylamide gels, and the proteins were subsequently transferred onto PVDF membranes (Millipore, Billerica, MA, USA). Primary antibodies against GPX4 (Abcam, 1:1000), VCAM-1 (Servicebio, 1:1000, Wuhan, China), VE-cadherin (Abcam, 1:1000), and β-actin (Sigma-Aldrich, 1:3000, Mo, USA) were used, followed by incubation with horseradish peroxidase-linked secondary antibodies (ProteinTech Group, Inc., HRP-goat anti-mouse, 1:5000; HRP-Goat Anti-Rabbit,1:5000, Wuhan, China). All samples were run in triplicate.

Extraction of RNA and Quantitative RT-PCR (qRT-PCR)

RNAiso Plus reagent (Takara Biotechnology, Dalian, China) was used to extract RNA from lung tissues. Complementary DNA was synthesized according to the manufacturer's protocol. qRT-PCR was performed using ChamQ Universal SYBR qPCR Master Mix (Vazyme Biotech, Nanjing, China). Target gene mRNA levels were normalized to endogenous β-actin expression and quantified using the $2^{-\Delta\Delta}$ct method. All samples were run in triplicate. The primer sequences used were as follows:

β-actin-F: 5′-CTGTATGCCTCTGGTCGTAC-3′
β-actin-R: 5′-TGATGTCACGCACGATTTCC-3′
HMOX1-F: 5′-GCCCCACCAAGTTCAAACAG-3′
HMOX1-R: 5′-GCTCCTCAAACAGCTCAATGT-3′
HIF-1α-F: 5′- CTGCCACTGCCACCACAACTG-3′
HIF-1α-R: 5′- TGCCACTGTATGCTGATGCCTTAG-3′
TIMP1-F: 5′- GCATCTCTGGCATCTGGCATCC-3′
TIMP1-R: 5′- CGCTGGTATAAGGTGGTCTCGTTG-3′
IL6-F: 5′- CGTGGAAATGAGAAAAGAGTTGTGC-3′
IL6-R: 5′- GGTACTCCAGAAGACCAGAGGA-3′

Statistical Analyses

Statistical analyses were performed using SPSS 26.0 (IBM, Armonk, NY, United States), Prism 7 (GraphPad, San Diego, CA, United States), and R. Data are displayed as the mean ± SEM. Statistical significance in experiments comparing only two groups was determined using two-tailed Student's *t*-test. One-way ANOVA was used for comparisons between multiple groups, followed by post hoc analysis using the Student-Newman-Keuls test. Statistical significance was set at $p < 0.05$.

Result

Identification of Ferroptosis-Related Differentially Expressed Genes in Sepsis-Induced Lung Injury Models

Expression data between the LPS and Control groups in the GSE130936 were analyzed using GEO2R. The cut-off criteria for DEGs dataset were set as $|\log_2 FC| > 1$ and $p_{adjusted} < 0.05$. Using these criteria, 460 genes were upregulated, and 525 genes were identified as downregulated, and these genes are displayed in a volcano plot (Figure 1A). Then, to explore the correlation between ferroptosis and SLI, 340 ferroptosis-related genes obtained from the FerrDb database were intersected with sepsis-associated DEGs, and 38 ferroptosis-related DEGs were obtained and are shown in a Venn diagram and heat map (Figure 1B and 1C), including 26 up-regulated and 12 down-regulated genes (Table 1).

Functional Enrichment Analyses and PPI Networks for Ferroptosis-Related Differentially Expressed Genes

In order to gain a better understanding of the functions of these genes, GO and KEGG analyses of 38 ferroptosis-related DEGs ($p < 0.05$) were performed using R software. As shown in Figure 2A and 2B, the response to hypoxemia was significantly enriched in the biological process category. Ferroptosis, autophagy, and HIF-1 signaling pathways were ranked among the top 20 KEGG pathways. Subsequently, ferroptosis-related DEGs were further analyzed to construct a PPI network (Figure 3). The Cytoscape software and MCODE were used to identify the most significant cluster (cluster 1, containing eight genes). Another GO and KEGG analysis were conducted on these eight genes (Table 2), and we found that four out of the eight genes in cluster 1 (IL-6, HMOX1, HIF-1α, and TIMP1) were enriched in the HIF-1 signaling pathway. These genes were then selected as candidate genes for further analysis and were identified as the key ferroptosis-related genes involved in sepsis-induced lung injury.

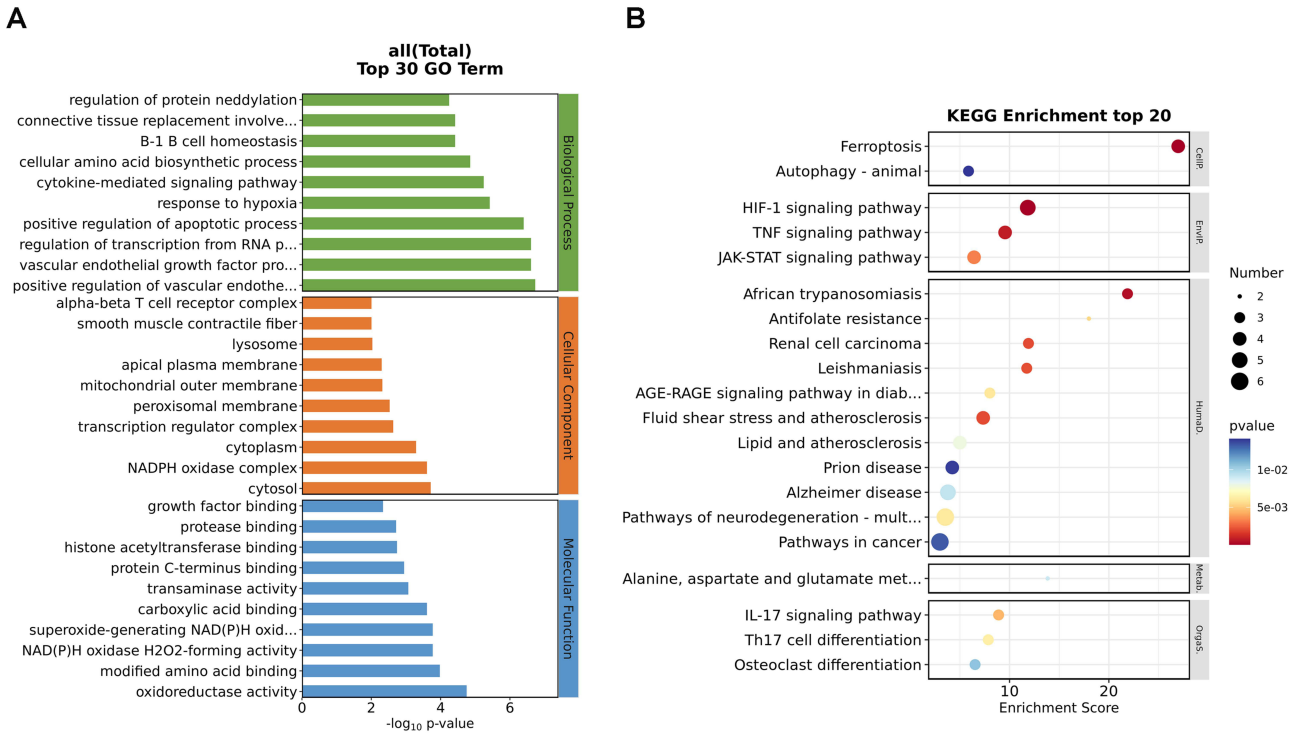

Figure 1 Identification of ferroptosis-related DEGs. (**A**) Volcano plots of DEGs. (**B**) Venn diagram of DEGs from GSE130936 and ferroptosis-related genes. (**C**) Heatmap of DEGs in GSE130936.

Table 1 Ferroptosis-Related Differentially Expressed Genes of Sepsis

Gene Symbol	Adj.P.Val	Log_2FC	ID	Gene Title
IL-6	2.04E-05	3.71	1450297_at	Interleukin 6
Timp1	4.96E-06	3.32	1460227_at	Tissue inhibitor of metalloproteinase 1
Slc39a14	3.23E-06	3.01	1427035_at	Solute carrier family 39 (zinc transporter), member 14
IL1b	1.16E-05	2.95	1449399_a_at	Interleukin 1 beta
Ndrg1	2.30E-05	2.66	1423413_at	N-myc downstream regulated gene 1
Ido1	3.98E-05	2.22	1420437_at	Indoleamine 2.3-dioxygenase 1
Hif1a	7.44E-05	2.15	1427418_a_at	Hypoxia inducible factor 1, alpha subunit
Ddit4	3.47E-04	1.82	1428306_at	DNA-damage-inducible transcript 4
Hmox1	4.40E-04	1.78	1448239_at	Heme oxygenase 1
Slc2a1	5.72E-05	1.73	1434773_a_at	Solute carrier family 2 (facilitated glucose transporter), member 1
Gpx2	8.83E-06	1.68	1449279_at	Glutathione peroxidase 2
Hamp	4.58E-04	1.51	1419196_at	Hepcidin antimicrobial peptide
Tnfaip3	5.30E-05	1.46	1450829_at	Tumor necrosis factor, alpha-induced protein 3
Pgd	4.05E-04	1.40	1436771_x_at	Phosphogluconate dehydrogenase
Psat1	2.33E-03	1.35	1451064_a_at	Phosphoserine aminotransferase 1
Cirbp	8.87E-03	1.23	1416332_at	Cold inducible RNA binding protein
Atf4	3.00E-03	1.22	1438992_x_at	Activating transcription factor 4
Socs1	1.60E-03	1.20	1450446_a_at	Suppressor of cytokine signaling 1
Ncf2	7.33E-04	1.15	1448561_at	Neutrophil cytosolic factor 2
Ptpn6	5.80E-04	1.12	1460188_at	Protein tyrosine phosphatase, non-receptor type 6
Txnrd1	3.69E-03	1.08	1421529_a_at	Thioredoxin reductase 1
Sat1	3.38E-03	1.07	1420502_at	Spermidine/spermine N1-acetyl transferase 1
Qsox1	7.82E-04	1.07	1420831_at	Quiescin Q6 sulfhydryl oxidase 1
Got1	3.75E-04	1.04	1450970_at	Glutamic-oxaloacetic transaminase 1, soluble
Asns	6.99E-03	1.04	1433966_x_at	Asparagine synthetase
Dusp1	4.83E-02	1.03	1448830_at	Dual specificity phosphatase 1
Ulk2	3.11E-03	−1.01	1417847_at	Unc-51 like kinase 2
Dpep1	2.05E-03	−1.05	1419674_a_at	Dipeptidase 1 (renal)
Mtch1	3.65E-04	−1.09	1460718_s_at	Mitochondrial carrier 1
Lpin1	1.84E-02	−1.10	1418288_at	Lipin 1
Pex6	1.42E-04	−1.21	1424078_s_at	Peroxisomal biogenesis factor 6
Fads1	2.46E-04	−1.22	1423680_at	Fatty acid desaturase 1
Acsl1	4.03E-03	−1.24	1423883_at	Acyl-CoA synthetase long-chain family member 1

(*Continued*)

Table 1 (Continued).

Gene Symbol	Adj.P.Val	Log_2FC	ID	Gene Title
Mmd	2.85E-04	−1.29	1423489_at	Monocyte to macrophage differentiation-associated
Epas1	2.54E-04	−1.42	1449888_at	Endothelial PAS domain protein 1
Lifr	9.83E-04	−1.87	1454984_at	Leukemia inhibitory factor receptor
Dpp4	9.09E-05	−2.06	1416697_at	Dipeptidylpeptidase 4
Nox4	3.13E-03	−2.10	1451827_a_at	NADPH oxidase 4

Verification of the Key Ferroptosis-Related Genes in Sepsis-Induced Lung Injury

Next, in order to observe whether the above four candidate ferroptosis-associated genes exhibits the same trend of changes in previous related experiments, we validated them by selecting GSE60088 and GSE137342 as the validation datasets. The mRNA levels of IL-6, TIMP1, HIF-1α, and HMOX1 were increased significantly in the lung tissues of mice induced by sepsis (Figure 4A) and in the plasma of septic patients (Figure 4B) compared with the control group.

Phloretin Protects Against LPS-Induced Lung Injury

We then searched the c-MAP database to identify potential small molecules or drugs that might affect DEGs related to ferroptosis during SLI (Table 3). Phloretin, a natural product derived from apple plants, was selected as a potential compound to alleviate SLI because of its excellent anti-inflammatory effects introduced above. Simultaneously, its target

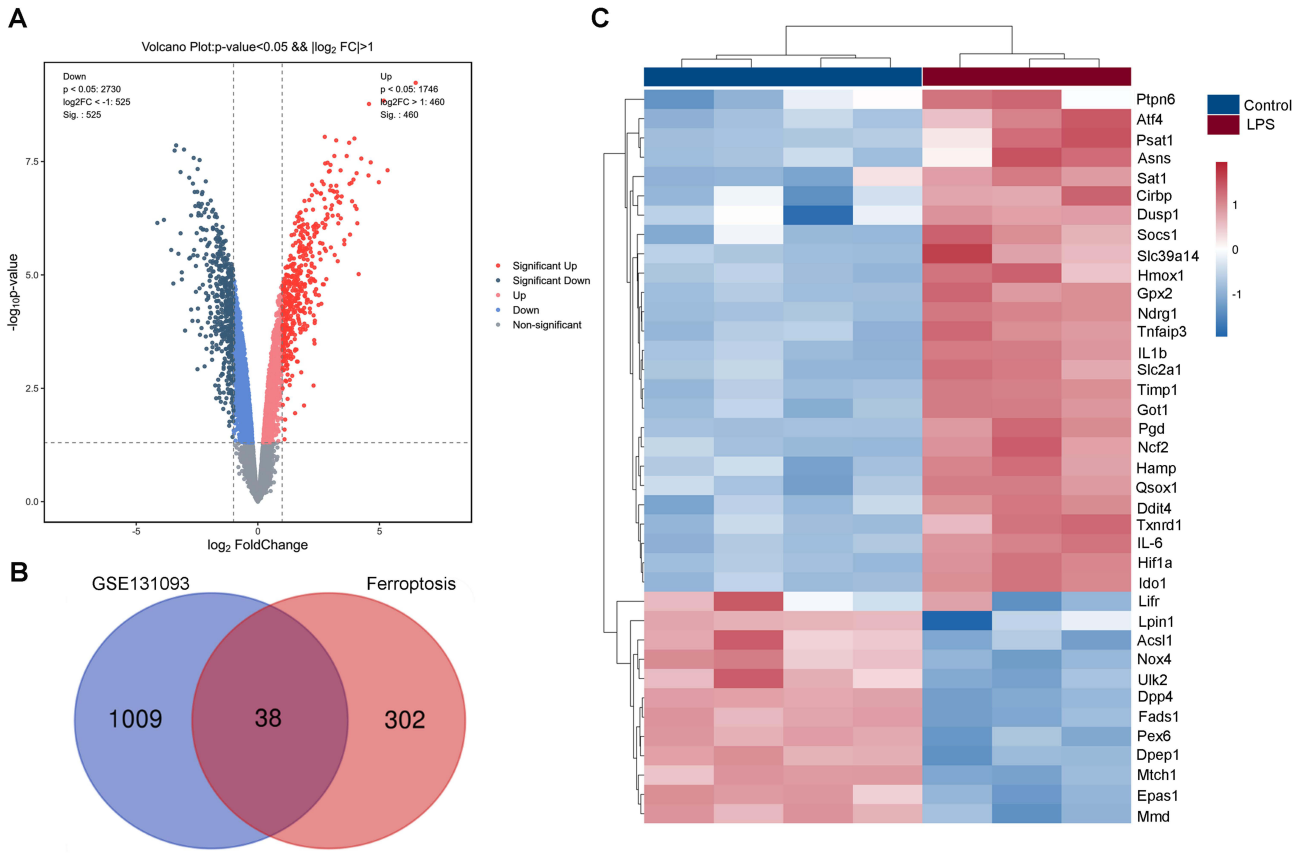

Figure 2 Enrichment analyses of ferroptosis-related DEGs. (**A**) Functions of ferroptosis-related DEGs with GO enrichment analysis. (**B**) Signaling pathways of ferroptosis-related DEGs with KEGG enrichment analysis.

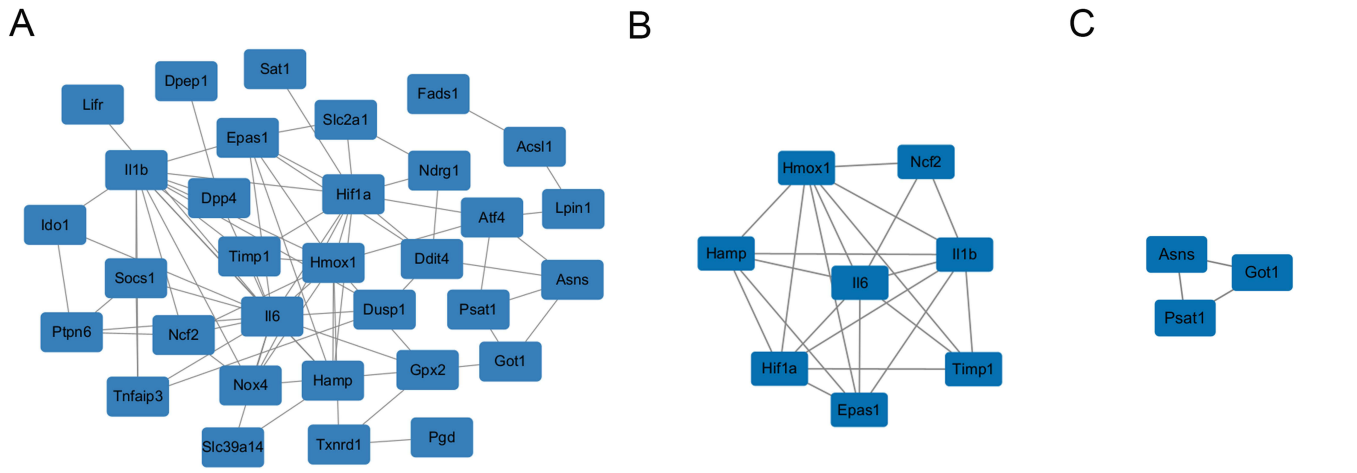

Figure 3 PPI analysis of ferroptosis-related DEGs. (**A**) PPI network of ferroptosis-related DEGs. (**B**) Gene cluster 1 based on the MCODE algorithm. **(C**) Gene cluster 2 based on the MCODE algorithm.

SLC23A1 is highly expressed in lung,[25] while AQP9's important pathophysiological role in sepsis has been identified,[26] which lead us to believe that PHL is a more reliable choice compared to other drugs filtered. To evaluate the affinity of the candidate substance for their target proteins, we performed molecular docking analysis. The binding poses and

Table 2 Functional Enrichment Analysis of Genes in Cluster 1

Ontology	ID	Description	Adj.P.Val	Gene ID
BP	GO:0002262	Myeloid cell homeostasis	6.03401E-07	Hmox1/Hif1a/Il6/Hamp/Epas1
BP	GO:0048771	Tissue remodeling	6.03401E-07	Timp1/Hif1a/Il6/Hamp/Epas1
BP	GO:0002246	Wound healing involved in inflammatory response	1.024E-06	Timp1/Hmox1/Hif1a
BP	GO:0043619	Regulation of transcription from RNA polymerase II promoter in response to oxidative stress	1.024E-06	Hmox1/Hif1a/Epas1
BP	GO:0055072	Iron ion homeostasis	1.9533E-06	Hmox1/Hif1a/Hamp/Epas1
CC	GO:0043020	NADPH oxidase complex	2.83E-02	Ncf2
CC	GO:0045179	Apical cortex	2.83E-02	Hamp
CC	GO:0016607	Nuclear speck	2.83E-02	Hif1a/Epas1
CC	GO:0030141	Secretory granule	3.27E-02	Il1b/Ncf2
CC	GO:0099738	Cell cortex region	5.36E-02	Hamp
MF	GO:0005125	Cytokine activity	1.21E-03	Timp1/Il6/Il1b
MF	GO:0001223	Transcription coactivator binding	1.69E-03	Hif1a/Epas1
MF	GO:0001221	Transcription coregulator binding	6.86E-03	Hif1a/Epas1
MF	GO:0008083	Growth factor activity	6.86E-03	Timp1/Il6
MF	GO:0070851	Growth factor receptor binding	6.86E-03	Il6/Il1b
KEGG	Mmu04066	HIF-1 signaling pathway	1.25E-04	Timp1/Hmox1/Hif1a/Il6
KEGG	Mmu04659	Th17 cell differentiation	3.15E-03	Hif1a/Il6/Il1b

(*Continued*)

Table 2 (Continued).

Ontology	ID	Description	Adj.P.Val	Gene ID
KEGG	Mmu05418	Fluid shear stress and atherosclerosis	5.27E-03	Hmox1/Il1b/Ncf2
KEGG	Mmu01523	Antifolate resistance	5.27E-03	Il6/Il1b
KEGG	Mmu05143	African trypanosomiasis	7.66E-03	Il6/Il1b

interactions of phloretin with IL-6, TIMP1, HIF-1α and HMOX1 were obtained with Autodock Vina v.1.2.2 and shown in Figure 5. As shown in Figure 6A–6D, qRT-PCR confirmed that IL-6, TIMP1, HIF-1α, and HMOX1 mRNA expression was upregulated in mouse lung tissues challenged with LPS compared to control mice, and PHL significantly inhibited the expression of four key genes. Histologically, LPS treatment resulted in edema, thickening of the alveolar wall, and neutrophil infiltration in the lung parenchyma; however, these effects were markedly inhibited by PHL treatment (Figure 6E and 6F). Existing literature has indicated that Vascular Endothelial cadherin (VE-cadherin) and Vascular Cellular Adhesion Molecule-1 (VCAM-1) are key in endothelial and epithelial pulmonary injury,[27,28] so we also included them in the observation indicators. PHL increased VE-cadherin and decreased VCAM-1 induced by LPS (Figure 6G and 6H). Serum levels of inflammatory factors IL-6 and TNF-α were also alleviated in PHL-treated mice challenged with LPS compared to those in the LPS group (Figure 6I and 6J).

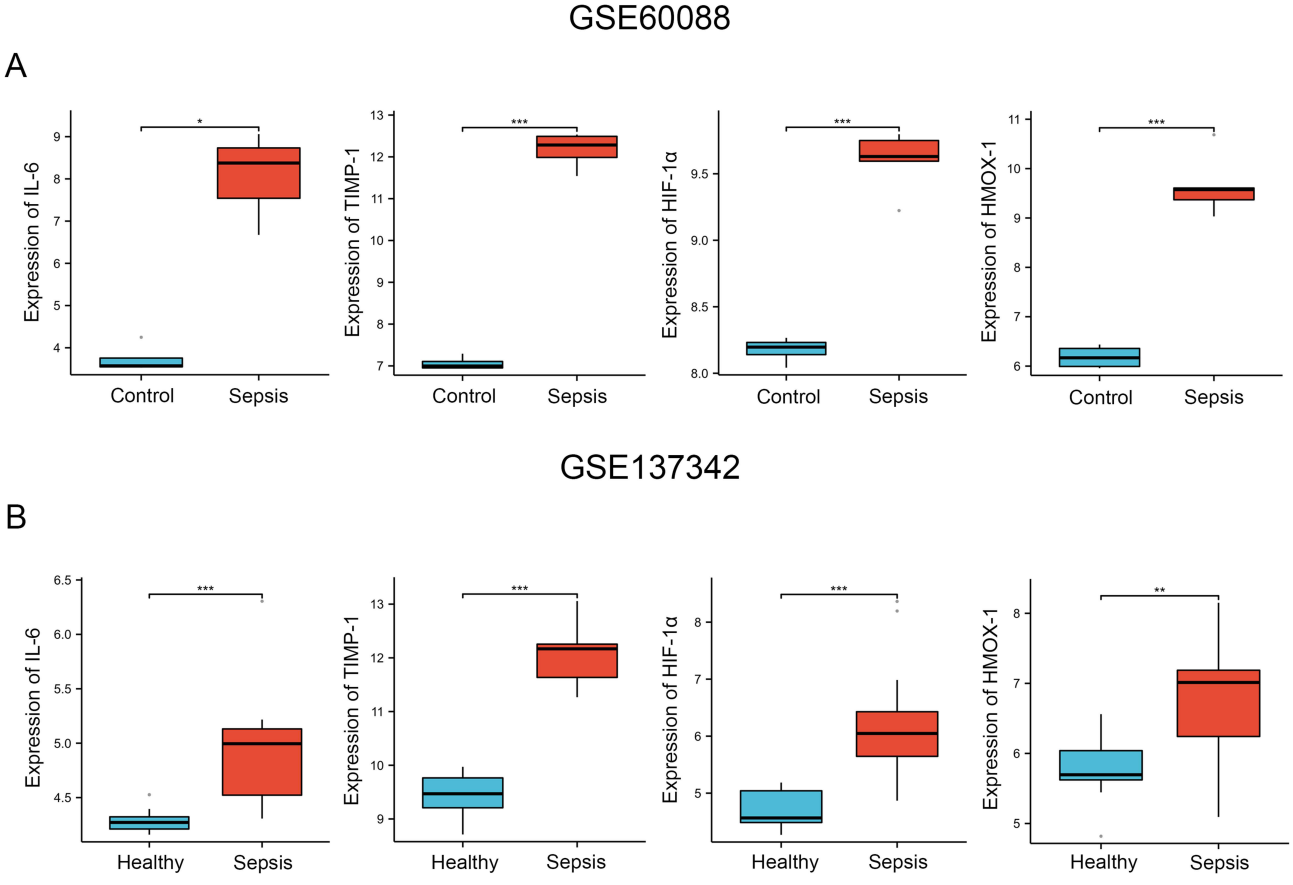

Figure 4 Verification of the four candidate genes (IL-6, TIMP1, HIF-1α, HMOX1) (**A**) in septic and control mice lung samples in GSE60088 dataset (**B**) and peripheral blood of healthy and septic patients in GSE137342. ***$p < 0.001$, **$p < 0.01$, *$p < 0.05$.

Table 3 Potential Small Molecules or Drugs That May Have Effect on Ferroptosis-Related DEGs Enriched by c-MAP

Pert_id	Pert_iname	Moa	Target_Name	Norm_cs
BRD-A37959677	Estrone	Estrogen receptor agonist|Estrogenic hormone	ESR1|ESR2	−1.85
BRD-K49372556	Mofezolac	Cyclooxygenase inhibitor	PTGS1	−1.77
BRD-K65503129	CCT-018159	HSP inhibitor	HSP90AA1|HSP90AB1	−1.68
BRD-K52751261	TAK-715	P38 MAPK inhibitor	MAPK14|TNF	−1.6
BRD-K15563106	Phloretin	Sodium channel inhibitor	AQP9|CLCN3|SLC23A1	−1.31
BRD-K17513304	Firategrast	Integrin inhibitor	ITGA4|ITGB1|ITGB7	−1.16
BRD-A30655177	LFM-A13	BTK inhibitor	BTK	−1.03
BRD-M80207679	Nemonapride	Dopamine receptor antagonist	DRD2|DRD3|DRD4	−0.84
BRD-K17849083	Tranilast	Angiogenesis inhibitor	IDO1|IFNG|IL10|IL2|IL4|SLC22A12|TGFB1|TNF|TRPV2|HPGDS|HRH1	−0.59
BRD-K14349461	Pyridoxine	Vitamin B	DDC|PDXK	−0.5

Phloretin Alleviated LPS-Stimulated Pulmonary Ferroptosis and Apoptosis

Finally, the effect of PHL on SLI and ferroptosis was evaluated. Western blot analysis of lung tissues revealed markedly higher levels of GPX4 in mice treated with PHL than those in the untreated group subjected to LPS (Figure 7A and 7B). Oxidative stress biomarkers, MDA and GSSG levels, were increased by LPS administration, whereas the results exhibited an obvious reduction in both MDA and GSSG levels following administration of PHL (Figure 7C and 7D). In addition, ferroptosis is closely related to apoptosis and oxidative stress.[29,30] 8-OHdG immunoreactivity was measured as an index of membrane lipid peroxidation and oxidative DNA damage. As shown in Figure 7E and 7F, significant increases in 8-OHdG-positive cells were observed in the LPS group compared with those in the control group. PHL significantly alleviated LPS-induced pulmonary oxidative stress, as indicated by the decreased 8-OHdG immunoreactivity in the lung tissues of septic mice. TUNEL, a universal assay for multiple cell death, including ferroptosis, confirmed the increase in lung tissues of LPS-administered mice, whereas the proportion of TUNEL-positive cells decreased in the LPS plus PHL group (Figure 7G and 7H). These findings demonstrated that PHL is a candidate compound that alleviates SLI by inhibiting ferroptosis through the regulation of IL-6, TIMP1, HIF-1α, and HMOX1.

Discussion

The lung is the most vulnerable organ in the development of sepsis, and almost half of patients with sepsis progress to ALI or ARDS.[31] Despite the constant developments in clinical diagnosis and treatment strategies, the prognosis of sepsis-associated ALI remains poor.

In recent years, ferroptosis has become a popular topic in the study of various diseases. According to latest studies, critical COVID-19 patients with higher levels of plasma MDA and catalytic iron have higher risk for 90-day mortality[32] while research on critical acute pancreatitis and non-alcoholic fatty liver disease patients reveal that the biomarker of ferroptosis at all stages is significantly higher in non-survival patients than that in the survival group.[33] Moreover, a study on multiple organ dysfunction syndrome (MODS) patients showed that the maximum value of MDA and catalytic iron per patient had a significant positive correlation with the sequential organ failure assessment (SOFA) score. MDA values were consistently higher in the deceased group when analyzed everyday,[34] indicating that in long-term ferroptosis may increase the risk of death in septic patients. The inhibition of ferroptosis is considered an effective treatment for sepsis. As the concrete mechanisms between ferroptosis and sepsis-induced ALI/ARDS has not been completely elucidated,[35,36] we recognized the urgency of identifying ferroptosis-related biomarkers and efficacious medications to prevent and treat SLI. In the current study, we identified 38 ferroptosis-related genes associated with BA. The HIF-1 signaling pathway

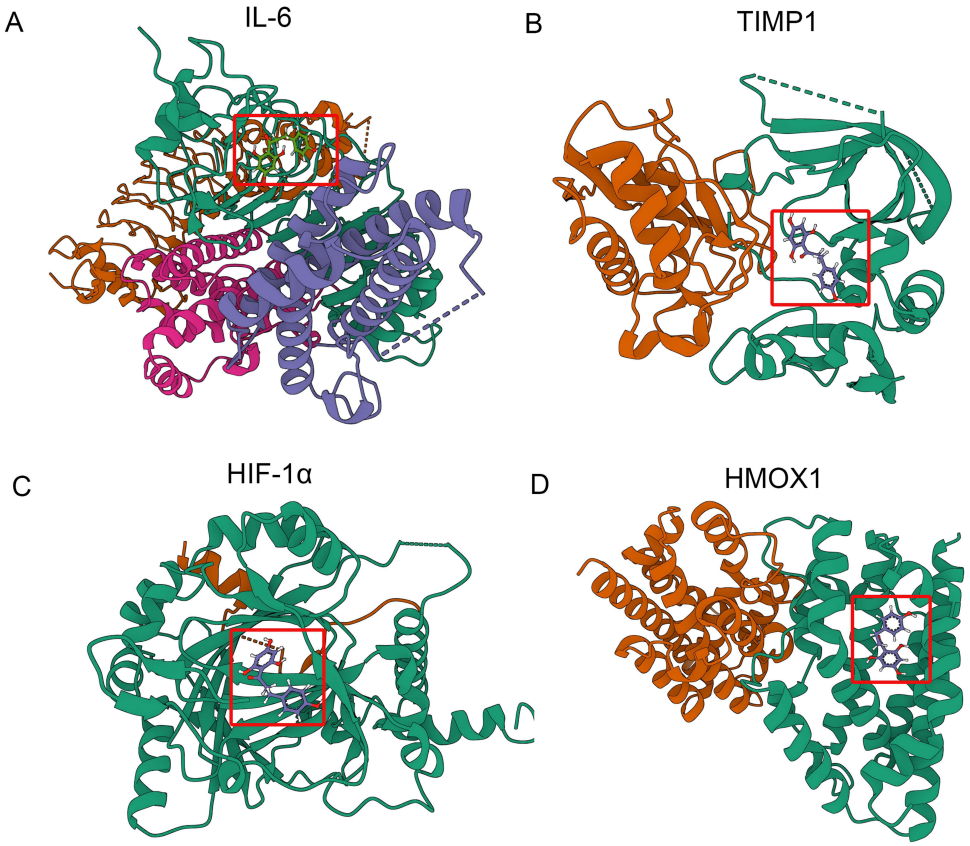

Figure 5 Binding mode of phloretin to their targets by molecular docking. (**A**–**D**) Docking mode of phloretin to IL-6, TIMP-1, HIF-1α, HMOX1. The crystal structure of phloretin is marked within the red square in each figure.

was one of the most significantly enriched pathways. HIF-1 is an oxygen-regulated transcriptional activator commonly the expression of HIF-1α surges in hypoxic cells.[37] HIF-1α is also involved in numerous diseases through diverse pathways. Dysregulation of Akt/mTOR/HIF-1 signaling has been observed in SARS-CoV-2 infection, suggesting an alternative therapy.[38] HIF-1α has been found to be an upstream regulator of BNIP3 in the hypoxia signaling pathway during myocardial ischemia-reperfusion injury.[39] Wu et al demonstrated that ferroptosis occurs in mouse models exposed to di-(2-ethylhexyl) phthalate (DEHP), a plasticizer, via the HIF-1α/HO-1 signaling pathway.[40] Therefore, we hypothesized that the HIF signaling pathway plays a significant role in SLI-induced ferroptosis. On account of more concrete clustering analysis results, we proposed that IL-6, TIMP1, HIF-1α and HMOX1 were key genes participated in ferroptosis regulation in SLI.

IL-6 is a 26-kD secreted protein relevant to inflammatory diseases.[41] Elevated IL-6 is usually seen in sepsis,[42] rheumatoid arthritis,[43] chronic obstructive pulmonary disease (COPD)[44] etc. Previous studies have shown that the expression of IL-6 is upregulated upon LPS-induced sepsis, which then amplifies STAT3 activation, leading to a vicious cycle of further IL-6 through TLR4/Mal signaling.[45] The therapeutic strategy mainly focuses on blocking monoclonal antibodies, and different inhibiting sites where IL-6 blockers act have been exhaustively summarized in the literature.[46] TIMP1 is a cancer-related chemokine associated with angiogenesis, cell survival, proliferation, and apoptosis.[47] TIMP1 is favorable for tumor progression in pancreatic cancer, as it promotes perineural invasion and triggers neutrophil extracellular traps (NETs) to promote tumorigenesis.[48,49] On the other hand, prior BA and experimental analyses have identified TIMP1 as an inflammatory biomarker in temporal lobe epilepsy.[50] Clinical research has also substantiated the connection between elevated serum TIMP1 levels, organ dysfunction, and mortality in septic patients.[51] As an adaptation to hypoxia, HIF-1α increases the production of harmful inflammatory cytokines, including TNF-α, IL-1, and IL-4, and promotes angiogenesis, glycolysis, and erythropoiesis.[52] HIF-1α is also known to mediate the

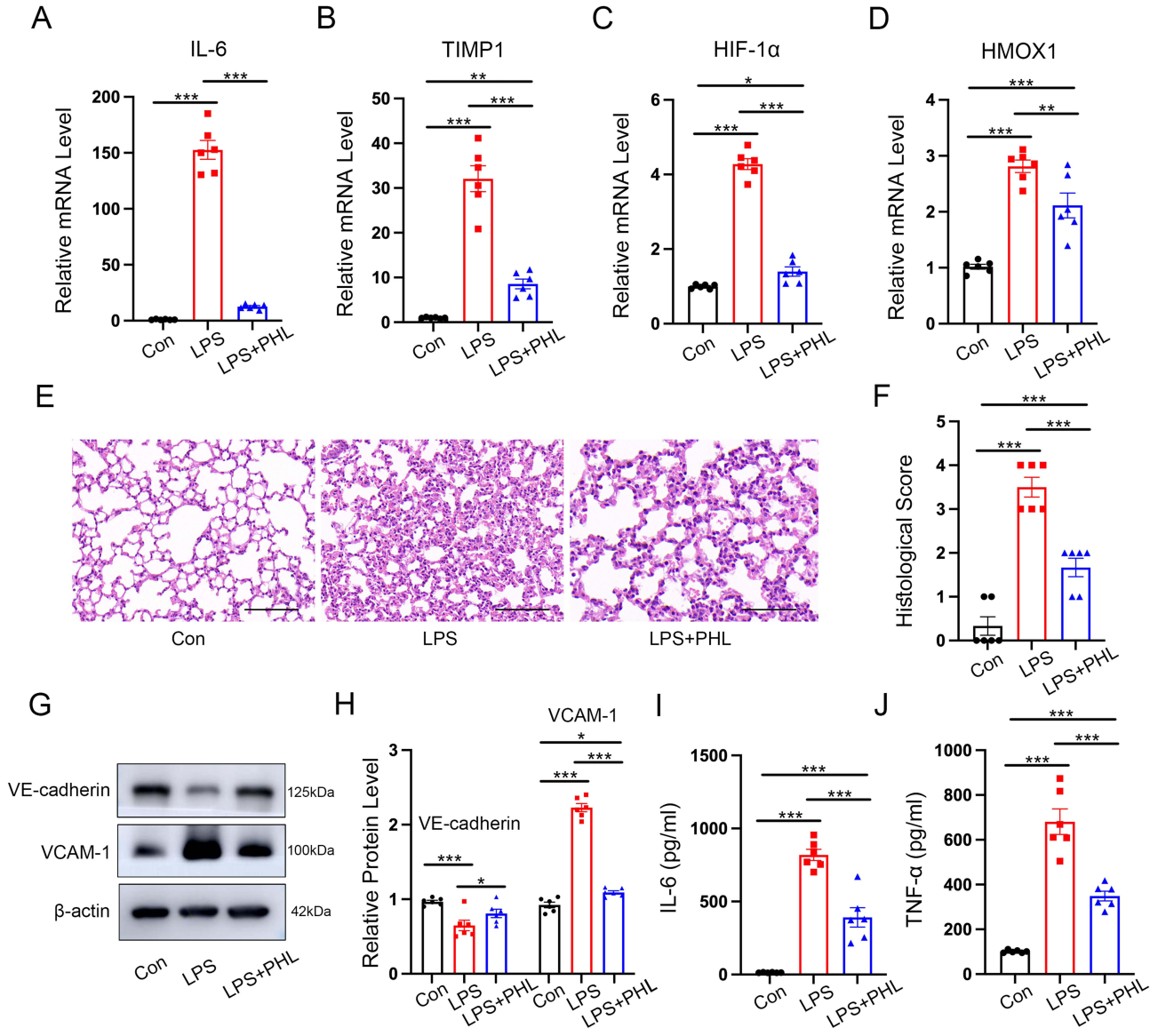

Figure 6 Therapeutic effects of phloretin on SLI mice. (**A**–**D**) Relative mRNA levels of IL-6, TIMP-1, HIF-1α, and HMOX1 in lung tissues of mice by qRT-PCR. (**E**) H&E staining of mice lung tissues (scale bar is 50 μm). (**F**) Lung injury scores. (**G** and **H**) The expression levels of VE-cadherin and VCAM-1 in lung tissues were evaluated semi-quantitatively by Western blot analysis. Representative bands (**G**) and corresponding histogram (**H**) were shown. (**I** and **J**) IL-6 and TNF-α level in serum. Data are represented as mean ± SEM (n=6 per group). ***$p < 0.001$, **$p < 0.01$, *$p < 0.05$.

inflammatory responses during LPS-induced sepsis.[53] Interestingly, enhanced HIF-1α expression differs under different conditions during ferroptosis. For instance, in cervical cancer, it leads to ferroptosis resistance,[54] while overactivation of HIF promotes ferroptosis in myocardial ischemia–reperfusion injury.[39] HMOX1 encodes heme oxygenase (HO), a stress-induced enzyme that catalyzes the process of heme degradation and exhibits anti-inflammatory effects in cardiovascular disease; metabolic disorders; and liver, kidney, and lung diseases.[55] In hind limb ischemia injury mouse models, HMOX1 influences both up-and downstream HIF-1α, and rescues ischemic injury by stabilizing HIF-1α. Similarly, the upregulation of HMOX1 due to excess production of heme is positively related to the degree of cardiac ferroptosis in sickle cell disease.[56] Such a correlation between HMOX1 and ferroptosis has also been observed in osteosarcoma[57] and diabetic atherosclerosis,[58] which indicates that flexible regulation of HMOX1 serves as a novel approach for the treatment of cancer and inflammatory diseases.

We established LPS-induced SLI mouse models to confirm the BA results and found that the expressions of IL-6, TIMP1, HIF-1α, and HMOX1 were significantly upregulated. We then used c-MAP, currently the largest database that

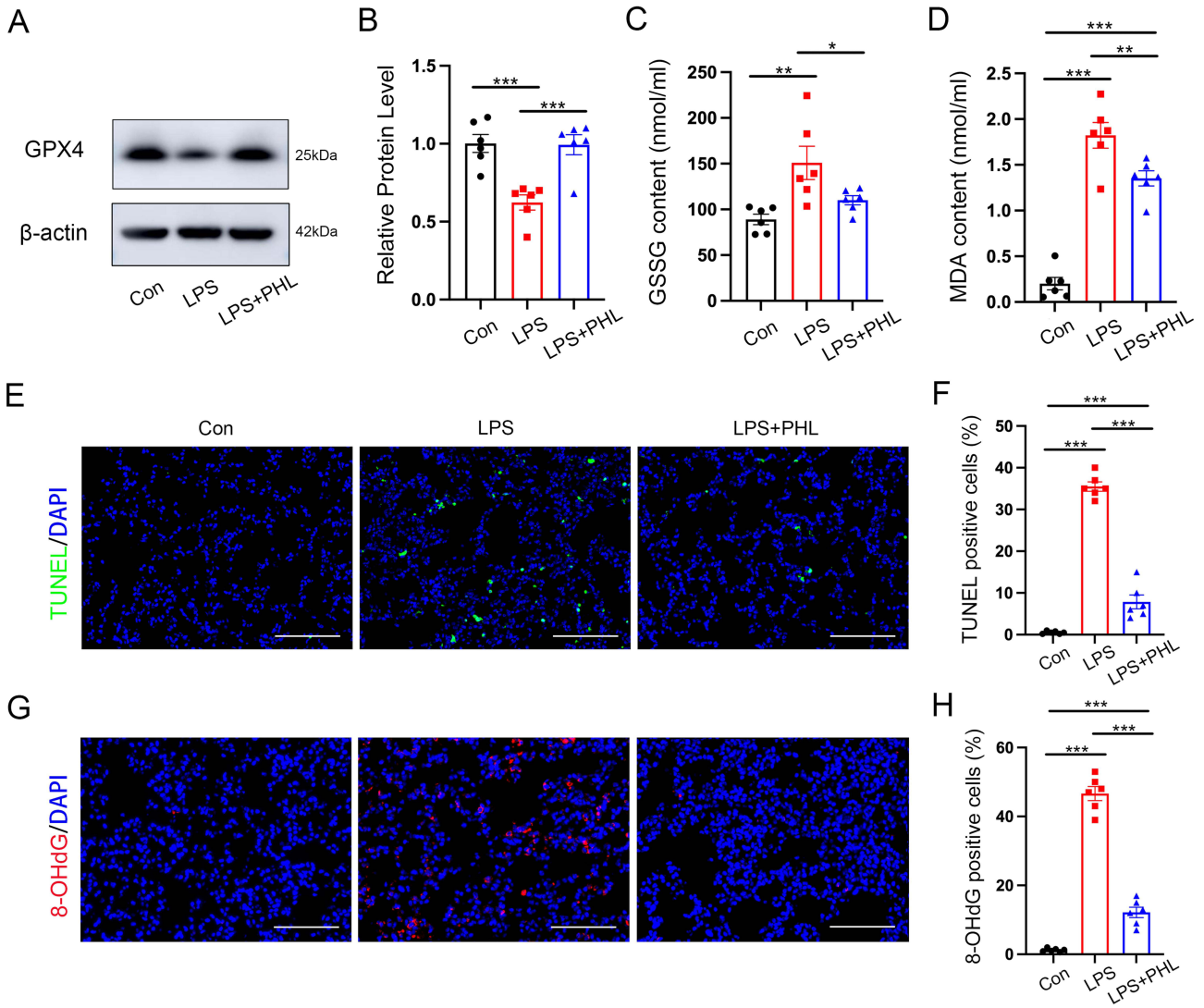

Figure 7 Effects of phloretin on LPS-stimulated pulmonary ferroptosis and apoptosis. (**A** and **B**) The expression levels of GPX4 in lung tissues was evaluated semi-quantitatively by Western blot analysis. Representative bands (**A**) and corresponding histogram (**B**) were shown. (**C** and **D**) MDA and GSSG levels were measured in serum of mice. (**E** and **F**) Lung tissues were stained with TUNEL (red). Nuclei were counterstained with 4'6-diamidino-2-phenylindole (DAPI) (blue). Percentages of $TUNEL^+$ cells are shown as histograms. (**G** and **H**) Lung tissues were stained with 8-OHdG (green), Nuclei were counterstained with DAPI (blue). Percentages of 8-OHdG-positive cells are shown as histograms. Data are represented as mean ± SEM (n=6 per group). ***$p < 0.001$, **$p < 0.01$, *$p < 0.05$.

connects related genes, drugs, and diseases,[59] to screen for possible natural medicines and verify its therapeutic effect on SLI mouse models. High-quality literature has summarized small molecules that target ferroptosis in vivo and clinical trials, and it differentiates targeted pathways and proposed mechanisms.[60] The side effects and off-target effects of conventional medicine or chemical agents are inevitable So more dietary and natural compounds may make up for this deficiency. Phloretin is one of the natural agents listed, and we chose it for its reported anti-inflammatory effects on lung injury.[17,61] Consistently, our study showed that phloretin decreased the expression of the four hub genes and ameliorated lung injury and inflammation in septic mice. VE-cadherin binds to adjacent lung endothelial cells and is important for basal lung microvascular stabilization.[62] Downregulation of VE-cadherin induced by IL-1β has been shown to be the basis for septic lung barrier impairment.[63] In contrast, VCAM-1 is responsible for leukocyte adhesion and extravasation is upregulated during inflammation. In PM2.5-induced lung injury, increased polymorphonuclear leukocytes (PMN) via upregulated VCAM-1 expression leads to exacerbated inflammation and injury.[46] In our phloretin treatment group, VE-cadherin and VCAM-1 were upregulated and downregulated, respectively, compared to the LPS group, which further confirmed the value of phloretin in SLI treatment. In addition, we verified for the first time that phloretin could improve

ferroptosis in SLI. This may lead to wider application of phloretin in other ferroptosis-related diseases. Since ferroptosis is related to oxidative stress and apoptosis,[64] immunofluorescence of TUNEL and 8-OHdG in lung tissue was performed, and the results fully illustrated the anti-ferroptosis effect of phloretin.

Four ferroptosis-related genes were identified to play important roles in SLI through BA and have been verified in other GEO datasets and animal models. In addition, we discovered a novel natural therapeutic compound by using the c-MAP tool. Identifying specific genes that are involved in ferroptosis and linking them to potential therapeutic compounds are novel aspects of our research. The use of a bioinformatics approach followed by experimental validation bridges computational predictions with practical, therapeutic insights. However, our study had several limitations. First, the experimental validation of human lung tissue is hindered by the difficulty in obtaining samples from patients with sepsis. Second, among the 38 ferroptosis-related genes, we focused only on four genes, leaving other genes to be explored comprehensively in the future. Third, we only adopted a single phloretin dosage in the study, and did not explore a dose-response relationship, which is crucial for therapeutic window and safety profile of phloretin. Thus, our results require further verification with more clinical data and tests and more in-depth and detailed exploration.

Conclusion

In conclusion, we identified key ferroptosis-related genes through a combination of bioinformatics analysis and experimental validation. Additionally, the natural compound phloretin significantly suppresses the expression of ferroptosis-related key genes, alleviates lung injury and inflammatory responses in LPS-induced SLI. These findings offer new strategies and theoretical support for the treatment of SLI.

Data Sharing Statement

The raw data supporting the conclusions of this article will be made available by the authors without any undue reservation.

Ethics Statement

The animal study and bioinformatic study involving human data (publicly available data) was approved by the Ethics Committee of the Xinhua Hospital, Shanghai Jiaotong University, School of Medicine (Permit number: XHEC-NSFC -2023-076).

Author Contributions

Zhile Li and Han Gan contributed equally to this work and should be considered as co-first authors. All authors made a significant contribution to the work reported, whether that is in the conception, study design, execution, acquisition of data, analysis and interpretation, or in all these areas; took part in drafting, revising or critically reviewing the article; gave final approval of the version to be published; have agreed on the journal to which the article has been submitted; and agree to be accountable for all aspects of the work.

Funding

This study was financially supported by grants from the National Natural Science Foundation of China LJ (No. 82072209) and the YQZ (No. 82302416).

Disclosure

The authors declare that this research was conducted in the absence of any commercial or financial relationships that could be construed as potential conflicts of interest.

References

1. Markwart R, Saito H, Harder T, et al. Epidemiology and burden of sepsis acquired in hospitals and intensive care units: a systematic review and meta-analysis. *Intensive Care Med*. 2020;46(8):1536–1551. doi:10.1007/s00134-020-06106-2
2. Gotts JE, Matthay MA. Sepsis: pathophysiology and clinical management. *BMJ*. 2016;i1585. doi:10.1136/bmj.i1585

3. Meyer NJ, Gattinoni L, Calfee CS. Acute respiratory distress syndrome. *Lancet*. 2021;398(10300):622–637. doi:10.1016/S0140-6736(21)00439-6
4. Zhang Y, Ning B. Signaling pathways and intervention therapies in sepsis. *Signal Transduct Target Ther*. 2021;6(1):407. doi:10.1038/s41392-021-00816-9
5. Tang D, Chen X, Kang R, Kroemer G. Ferroptosis: molecular mechanisms and health implications. *Cell Res*. 2021;31(2):107–125. doi:10.1038/s41422-020-00441-1
6. Jiang X, Stockwell BR, Conrad M. Ferroptosis: mechanisms, biology and role in disease. *Nat Rev Mol Cell Biol*. 2021;22(4):266–282. doi:10.1038/s41580-020-00324-8
7. Chen X, Kang R, Kroemer G, Tang D. Ferroptosis in infection, inflammation, and immunity. *J Exp Med*. 2021;218(6):e20210518. doi:10.1084/jem.20210518
8. Liu P, Feng Y, Li H, et al. Ferrostatin-1 alleviates lipopolysaccharide-induced acute lung injury via inhibiting ferroptosis. *Cell Mol Biol Lett*. 2020;25(1):10. doi:10.1186/s11658-020-00205-0
9. Wang X, Wang Y, Huang D, et al. Astragaloside IV regulates the ferroptosis signaling pathway via the Nrf2/SLC7A11/GPX4 axis to inhibit PM2.5-mediated lung injury in mice. *Int Immunopharmacol*. 2022;112:109186. doi:10.1016/j.intimp.2022.109186
10. Zhang H, Liu J, Zhou Y, et al. Neutrophil extracellular traps mediate m 6 A modification and regulates sepsis-associated acute lung injury by activating ferroptosis in alveolar epithelial cells. *Int J Biol Sci*. 2022;18(8):3337–3357. doi:10.7150/ijbs.69141
11. Wang YM, Gong FC, Qi X, et al. Mucin 1 Inhibits Ferroptosis and Sensitizes Vitamin E to Alleviate Sepsis-Induced Acute Lung Injury through GSK3β/Keap1-Nrf2-GPX4 Pathway. In: Zhou J. editor. *Oxid Med Cell Longev* 2022;2022:1–29. doi: 10.1155/2022/2405943
12. Wang Y, Chen D, Xie H, et al. AUF1 protects against ferroptosis to alleviate sepsis-induced acute lung injury by regulating NRF2 and ATF3. *Cell Mol Life Sci*. 2022;79(5):228. doi:10.1007/s00018-022-04248-8
13. Shi J, Song S, Wang Y, et al. Esketamine alleviates ferroptosis-mediated acute lung injury by modulating the HIF-1α/HO-1 pathway. *Int Immunopharmacol*. 2024;142:113065. doi:10.1016/j.intimp.2024.113065
14. Li J, Hu Y, Liang X, Liu M. Sodium Houttuyniae attenuates ferroptosis by regulating TRAF6-c-Myc signaling pathways in lipopolysaccharide-induced acute lung injury (ALI). *BMC Pharmacol Toxicol*. 2024;25(1):63. doi:10.1186/s40360-024-00787-x
15. Zhang Z, Li X, Guo J, et al. β-aminoisobutyrics acid, a metabolite of BCAA, activates the AMPK/Nrf-2 pathway to prevent ferroptosis and ameliorates lung ischemia-reperfusion injury. *Mol Med*. 2023;29(1):164. doi:10.1186/s10020-023-00729-z
16. Habtemariam S. The Molecular Pharmacology of Phloretin: anti-Inflammatory Mechanisms of Action. *Biomedicines*. 2023;11(1):143. doi:10.3390/biomedicines11010143
17. Huang WC, Lai CL, Liang YT, Hung HC, Liu HC, Liou CJ. Phloretin attenuates LPS-induced acute lung injury in mice via modulation of the NF-κB and MAPK pathways. *Int Immunopharmacol*. 2016;40:98–105. doi:10.1016/j.intimp.2016.08.035
18. Werner T. Bioinformatics applications for pathway analysis of microarray data. *Curr Opin Biotechnol*. 2008;19(1):50–54. doi:10.1016/j.copbio.2007.11.005
19. Liu C, Li Z, Xi H. Bioinformatics analysis and in vivo validation of ferroptosis-related genes in ischemic stroke. *Front Pharmacol*. 2022;13:940260. doi:10.3389/fphar.2022.940260
20. Li XZ, Xiong ZC, Zhang SL, et al. Potential ferroptosis key genes in calcific aortic valve disease. *Front Cardiovasc Med*. 2022;9:916841. doi:10.3389/fcvm.2022.916841
21. Long SW, Li SH, Li J, et al. Identification of osteoporosis ferroptosis-related markers and potential therapeutic compounds based on bioinformatics methods and molecular docking technology. *BMC Med Genom*. 2024;17(1):99. doi:10.1186/s12920-024-01872-0
22. Morris GM, Huey R, Olson AJ. Using AutoDock for Ligand-Receptor Docking. *Curr Protoc Bioinform*. 2008;24(1):8–14.
23. Wang Y, Bryant SH, Cheng T, et al. PubChem BioAssay: 2017 update. *Nucleic Acids Res*. 2017;45(D1):D955–D963. doi:10.1093/nar/gkw1118
24. Zhang H, Dong W, Li S, et al. Salidroside protects against ventilation-induced lung injury by inhibiting the expression of matrix metalloproteinase-9. *Pharm Biol*. 2021;59(1):758–766. doi:10.1080/13880209.2021.1967409
25. Bã M. The sodium-dependent ascorbic acid transporter family SLC23. *Mol Aspects Med*. 2013;34(2–3):436–454.
26. Da Silva IV, Garra S, Calamita G, Soveral G. The Multifaceted Role of Aquaporin-9 in Health and Its Potential as a Clinical Biomarker. *Biomolecules*. 2022;12(7):897. doi:10.3390/biom12070897
27. Spadaro S, Fogagnolo A, Campo G, et al. Markers of endothelial and epithelial pulmonary injury in mechanically ventilated COVID-19 ICU patients. *Crit Care*. 2021;25(1):74. doi:10.1186/s13054-021-03499-4
28. Su Y, Lucas R, Fulton DJR, Verin AD. Mechanisms of pulmonary endothelial barrier dysfunction in acute lung injury and acute respiratory distress syndrome. *Chin Med J Pulm Crit Care Med*. 2024;2(2):80–87. doi:10.1016/j.pccm.2024.04.002
29. Lee YS, Lee DH, Choudry HA, Bartlett DL, Lee YJ. Ferroptosis-Induced Endoplasmic Reticulum Stress: cross-talk between Ferroptosis and Apoptosis. *Mol Cancer Res*. 2018;16(7):1073–1076. doi:10.1158/1541-7786.MCR-18-0055
30. Yu Y, Yan Y, Niu F, et al. Ferroptosis: a cell death connecting oxidative stress, inflammation and cardiovascular diseases. *Cell Death Discov*. 2021;7(1):193. doi:10.1038/s41420-021-00579-w
31. Villar J, Sulemanji D, Kacmarek RM. The acute respiratory distress syndrome: incidence and mortality, has it changed? *Curr Opin Crit Care*. 2014;20(1):3–9. doi:10.1097/MCC.0000000000000057
32. Peleman C, Van Coillie S, Ligthart S, et al. Ferroptosis and pyroptosis signatures in critical COVID-19 patients. *Cell Death Differ*. 2023;30(9):2066–2077. doi:10.1038/s41418-023-01204-2
33. Deng Y. Serum iron fluctuations link ferroptosis process with mortality and prognosis of acute pancreatitis. *iScience*. 2023;26(10):7774. doi:10.1016/j.isci.2023.107774
34. Coillie SV. Targeting ferroptosis protects against experimental (multi)organ dysfunction and death. *Nat Commun*. 2022;13(1):1046. doi:10.1038/s41467-022-28718-6
35. Qu M, Zhang H, Chen Z, et al. The Role of Ferroptosis in Acute Respiratory Distress Syndrome. *Front Med*. 2021;8:651552. doi:10.3389/fmed.2021.651552
36. Liu X. The role of ferroptosis in acute lung injury. *Mol Cell Biochem*. 2022;477(5):1453–1461.
37. Semenza GL. HIF-1 and mechanisms of hypoxia sensing. *Current Opinion in Cell Biology*. 2001;13(2):167–171. doi:10.1016/S0955-0674(00)00194-0
38. Appelberg S, Gupta S, Svensson Akusjärvi S, et al. Dysregulation in Akt/mTOR/HIF-1 signaling identified by proteo-transcriptomics of SARS-CoV-2 infected cells. *Emerg Microbes Infect*. 2020;9(1):1748–1760. doi:10.1080/22221751.2020.1799723

39. Zhang Y, Liu D, Hu H, Zhang P, Xie R, Cui W. HIF-1α/BNIP3 signaling pathway-induced-autophagy plays protective role during myocardial ischemia-reperfusion injury. *Biomed Pharmacother*. 2019;120:109464. doi:10.1016/j.biopha.2019.109464
40. Wu Y, Wang J, Zhao T, et al. Di-(2-ethylhexyl) phthalate exposure leads to ferroptosis via the HIF-1α/HO-1 signaling pathway in mouse testes. *J Hazard Mater*. 2022;426:127807. doi:10.1016/j.jhazmat.2021.127807
41. Kang S, Narazaki M, Metwally H, Kishimoto T. Historical overview of the interleukin-6 family cytokine. *J Exp Med*. 2020;217(5):e20190347. doi:10.1084/jem.20190347
42. Hack C, De Groot E, Felt-Bersma R, et al. Increased plasma levels of interleukin-6 in sepsis [see comments]. *Blood*. 1989;74(5):1704–1710. doi:10.1182/blood.V74.5.1704.1704
43. Chung SJ, Kwon YJ, Park MC, Park YB, Lee SK. The Correlation between Increased Serum Concentrations of Interleukin-6 Family Cytokines and Disease Activity in Rheumatoid Arthritis Patients. *Yonsei Med J*. 2011;52(1):113. doi:10.3349/ymj.2011.52.1.113
44. Celli BR, Locantore N, Yates J, et al. Inflammatory Biomarkers Improve Clinical Prediction of Mortality in Chronic Obstructive Pulmonary Disease. *Am J Respir Crit Care Med*. 2012;185(10):1065–1072. doi:10.1164/rccm.201110-1792OC
45. Greenhill CJ, Rose-John S, Lissilaa R, et al. IL-6 Trans -Signaling Modulates TLR4-Dependent Inflammatory Responses via STAT3. *J Immunol*. 2011;186(2):1199–1208. doi:10.4049/jimmunol.1002971
46. Kaur S, Bansal Y, Kumar R, Bansal G. A panoramic review of IL-6: structure, pathophysiological roles and inhibitors. *Bioorg Med Chem*. 2020;28(5):115327. doi:10.1016/j.bmc.2020.115327
47. Jung KK, Liu XW, Chirco R, Fridman R, Kim HRC. Identification of CD63 as a tissue inhibitor of metalloproteinase-1 interacting cell surface protein. *EMBO J*. 2006;25(17):3934–3942. doi:10.1038/sj.emboj.7601281
48. Schoeps B, Eckfeld C, Prokopchuk O, et al. TIMP1 Triggers Neutrophil Extracellular Trap Formation in Pancreatic Cancer. *Cancer Res*. 2021;81(13):3568–3579. doi:10.1158/0008-5472.CAN-20-4125
49. Tian Z, Ou G, Su M, et al. TIMP1 derived from pancreatic cancer cells stimulates Schwann cells and promotes the occurrence of perineural invasion. *Cancer Lett*. 2022;546:215863. doi:10.1016/j.canlet.2022.215863
50. He Y, Zhang H, Ma L, et al. Identification of TIMP1 as an inflammatory biomarker associated with temporal lobe epilepsy based on integrated bioinformatics and experimental analyses. *J Neuroinflammation*. 2023;20(1):151. doi:10.1186/s12974-023-02837-3
51. Jones TK, Reilly JP, Anderson BJ, et al. Elevated Plasma Levels of Matrix Metalloproteinase-3 and Tissue-Inhibitor of Matrix Metalloproteinases-1 Associate With Organ Dysfunction and Mortality in Sepsis. *Shock*. 2022;57(1):41–47. doi:10.1097/SHK.0000000000001833
52. Scholz CC, Taylor CT. Targeting the HIF pathway in inflammation and immunity. *Curr Opin Pharmacol*. 2013;13(4):646–653. doi:10.1016/j.coph.2013.04.009
53. Peyssonnaux C, Cejudo-Martin P, Doedens A, Zinkernagel AS, Johnson RS, Nizet V. Cutting Edge: essential Role of Hypoxia Inducible Factor-1α in Development of Lipopolysaccharide-Induced Sepsis. *J Immunol*. 2007;178(12):7516–7519. doi:10.4049/jimmunol.178.12.7516
54. Xiong J, Nie M, Fu C, et al. Hypoxia Enhances HIF1α Transcription Activity by Upregulating KDM4A and Mediating H3K9me3, Thus Inducing Ferroptosis Resistance in Cervical Cancer Cells. In: Papaccio G. editor. *Stem Cells Int* 2022; 2022:1–16. doi: 10.1155/2022/1608806
55. Ryter SW. Heme Oxygenase-1: an Anti-Inflammatory Effector in Cardiovascular, Lung, and Related Metabolic Disorders. *Antioxidants*. 2022;11(3):555. doi:10.3390/antiox11030555
56. Menon AV, Liu J, Tsai HP, et al. Excess heme upregulates heme oxygenase 1 and promotes cardiac ferroptosis in mice with sickle cell disease. *Blood*. 2022;139(6):936–941. doi:10.1182/blood.2020008455
57. Lin H, Chen X, Zhang C, et al. EF24 induces ferroptosis in osteosarcoma cells through HMOX1. *Biomed Pharmacother*. 2021;136:111202. doi:10.1016/j.biopha.2020.111202
58. Meng Z, Liang H, Zhao J, et al. HMOX1 upregulation promotes ferroptosis in diabetic atherosclerosis. *Life Sci*. 2021;284:119935. doi:10.1016/j.lfs.2021.119935
59. Fang S, Dong L, Liu L, et al. HERB: a high-throughput experiment- and reference-guided database of traditional Chinese medicine. *Nucleic Acids Res*. 2021;49(D1):D1197–D1206. doi:10.1093/nar/gkaa1063
60. Sun S, Shen J, Jiang J, Wang F, Min J. Targeting ferroptosis opens new avenues for the development of novel therapeutics. *Signal Transduct Target Ther*. 2023;8(1):372. doi:10.1038/s41392-023-01606-1
61. Songyang Y, Li W, Li W, Yang J, Song T. The inhibition of GLUT1-induced glycolysis in macrophage by phloretin participates in the protection during acute lung injury. *Int Immunopharmacol*. 2022;110:109049. doi:10.1016/j.intimp.2022.109049
62. Matthay MA, Zemans RL, Zimmerman GA, et al. Acute respiratory distress syndrome. *Nat Rev Dis Primer*. 2019;5(1):18. doi:10.1038/s41572-019-0069-0
63. Xiong S, Hong Z, Huang LS, et al. IL-1β suppression of VE-cadherin transcription underlies sepsis-induced inflammatory lung injury. *J Clin Invest*. 2020;130(7):3684–3698. doi:10.1172/JCI136908
64. Wang Z, Chen X, Liu N, et al. A Nuclear Long Non-Coding RNA LINC00618 Accelerates Ferroptosis in a Manner Dependent upon Apoptosis. *Mol Ther*. 2021;29(1):263–274. doi:10.1016/j.ymthe.2020.09.024